

Heteronuclear Multidimensional NMR Spectroscopy of Solubilized Membrane Proteins: Resonance Assignment of Native Bacteriorhodopsin

Mario Schubert,^[a] Michael Kolbe,^[b, c] Brigitte Kessler,^[b] Dieter Oesterhelt,^[b] and Peter Schmieder^{*[a]}

Dedicated to Prof. Dr. Reiner Radeaglia on the occasion of his 65th birthday

KEYWORDS:

G-protein-coupled receptors · membrane proteins · NMR spectroscopy · triple resonance · TROSY

Resonance assignment is an essential first step in all NMR spectroscopy investigations, independent of whether structural or dynamic information is extracted from the spectra. In proteins, resonance assignment is performed by using the strategy of sequence-specific assignment, whereby the neighborhood of amino acid spin systems is established from the spectra. Pairs, triplets or longer stretches of spin systems are subsequently matched to the amino acid sequence and spin systems are thus assigned to amino acids. Originally, the assignment was accomplished by using homonuclear two-dimensional spectra (NOESY, DQF-COSY, TOCSY) and the method was limited to small proteins.^[1] Presently, a sequence-specific assignment based on triple resonance techniques^[2] that require proteins uniformly labeled with carbon-13 and nitrogen-15^[3] is typically preferred. The size of the proteins for which an assignment and a subsequent extraction of structural information can be achieved has thus been substantially increased. More recently, the size limit for proteins that can be studied by using solution-state NMR spectroscopy has been extended further by two novel

developments, namely the deuteration of proteins^[4] to enhance the relaxation properties of the carbon nuclei and the TROSY technique^[5] to enhance the relaxation properties of the amide protons and nitrogen nuclei.

Membrane proteins may not be larger than proteins that have already been analyzed in detail by solution-state NMR spectroscopy but the need for suitable solubilization increases the effective molecular weight substantially. Utilization of recently developed techniques, however, makes investigation of membrane proteins with solution-state NMR spectroscopy possible.^[6] A resonance assignment and the determination of two β -barrel membrane protein structures have been demonstrated.^[7]

Here we report the application of the new techniques to bacteriorhodopsin (BR), an archaeal membrane protein with a seven-transmembrane-helix (7TM) topology.^[8] BR shares its topology with an important class of eukaryotic membrane proteins, the G-protein-coupled receptors (GPCRs), and has long been used as a model system for biophysical investigation of this class of proteins,^[9] in particular since structural information on GPCRs at atomic resolution has only recently become available.^[10] The structure and dynamics of the loop regions that connect transmembrane helices are of importance for understanding GPCR function, since loop regions are responsible for the interaction of the receptor with ligands or the G-protein. Information about the loops is sometimes not available even in high-resolution X-ray structures.^[10, 11] Solution state NMR spectroscopy might therefore help provide the missing information. We report here a resonance assignment of the BR loop regions as a first step in the determination of their three-dimensional structure.


Bacteriorhodopsin was produced and solubilized in dodecyl-maltoside (DM) detergent micelles as described previously. The integrity of the samples was monitored by UV spectroscopy.^[12] It has been shown that bacteriorhodopsin solubilized in DM micelles yields NMR spectroscopy samples that are stable over extended periods of time, even when measured at elevated temperatures.^[13] All measurements could therefore be performed at 323 K, which significantly improved the linewidth of the resonances compared to those observed at room temperature. Two different labeling schemes were used: sample one was 100% doubly labeled with deuterium and nitrogen-15 and sample two was triply labeled with deuterium, carbon-13, and nitrogen-15, all to 100%. To minimize artifacts in the spectra, DM with a deuterated aliphatic tail was used for solubilization.

A complete exchange of deuterium against protons was unlikely since the samples were produced in D₂O and only transferred into H₂O for the solubilization in DM. It was expected that mainly the loops and solvent accessible parts of the transmembrane regions would be visible in the spectra, all of which were recorded with pulse sequences that utilized detection of the amide protons. Sample one was used to record ¹H,¹⁵N correlations with high resolution, three-dimensional ¹⁵N-edited NOESY spectra, and ¹⁵N relaxation experiments, while sample two was used to record three pairs of three-dimensional TROSY-based triple resonance experiments, namely HNCA/HN(CO)CA, HNCO/HN(CA)CO, and HNCACB/HN(CO)CACB (see the Experimental Section).^[14, 15]

[a] Dr. P. Schmieder, M. Schubert
Forschungsinstitut für Molekulare Pharmakologie
Robert-Rössle-Strasse 10
13125 Berlin (Germany)
Fax (+49) 30-94793-230
E-mail: schmieder@fmp-berlin.de

[b] Dr. M. Kolbe, B. Kessler, Prof. Dr. D. Oesterhelt
Max-Planck-Institut für Biochemie
Am Klopferspitz 18a
82152 Martinsried (Germany)

[c] Dr. M. Kolbe
Current address:
Max-Delbrück-Center for Molecular Medicine
Department of Crystallography
Robert-Rössle-Strasse 10
13125 Berlin (Germany)

 Supporting information for this article is available on the WWW under <http://www.chembiochem.org> or from the author.

A comparison between the ^{15}N HSQC (recorded by using a WATERGATE sequence^[16] and no sensitivity enhancement^[17]) and the ^{15}N TROSY experiments^[18] performed on the sample of BR 100% labeled with ^2H and ^{15}N is shown in Figure 1. While the intensity of most lines in the spectra are comparable, the line-width of both the proton and the ^{15}N lines in the TROSY spectrum are significantly smaller. Note that measurements were conducted in the dark. BR was therefore in the dark-adapted state, which represents a mixture of two retinal conformations, one with the retinal chromophore in the all-*trans*, 15-*anti* configuration, the other with the retinal chromophore in the 13-*cis*, 15-*syn* configuration.^[19] As a consequence, two sets of signals can be expected for residues close to the chromophore, which further increases the complexity of the spectra.

A comparison between the conventional and TROSY-type triple resonance experiments shows the clear advantage of the TROSY-based sequences (Figure 2). In particular, resonances in the more rigid parts of the molecules are absent in spectra recorded by using conventional pulse sequences. Not all triple resonance experiments that used the TROSY technique were of the same sensitivity, however. As has been reported previously, the high field used to optimize the TROSY effect causes problems with enhanced relaxation of the carbonyl resonances as a result of chemical shift anisotropy relaxation.^[20] Therefore, experiments with the carbonyl nucleus as a relay nucleus turned out to be less effective than those without a relay step, though not useless. The same was true for experiments where the α carbon nucleus was used as a relay nucleus, even though deuterium decoupling was applied. The assignment was therefore accomplished by using mainly the HNCA experiment, supported by the HN(CO)CA and

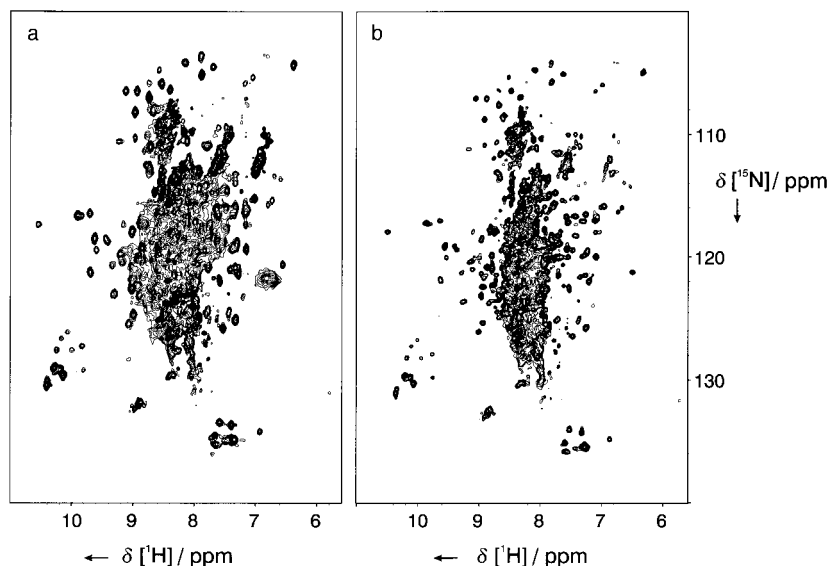


Figure 1. Comparison between an ^{15}N HSQC (a) and an ^{15}N TROSY spectrum (b) of $^2\text{H}/^{15}\text{N}$ -labeled BR. Both spectra were acquired in 15 h by using 48 scans and were processed identically. Note that signals from NH_2 or NH_3 moieties are missing in the spectrum recorded with the TROSY sequence.

the HNCO/HN(CA)CO pair when possible. In addition, the ^{15}N -edited NOESY spectra proved to be quite helpful. Chemical shifts of the β carbon nuclei were obtained in several cases from HNCACB experiments and chemical shifts of the carbonyl carbon nuclei from HNCO experiments. The C_α and the available C_β shifts were used to predict the amino acid type with the program type_prob^[21] and a sequence-specific assignment was performed in the conventional manner,^[22] supported by the program seq_prob.^[21] An example of the assignment procedure with strips from HNCA and HN(CO)CA is shown in Figure 3 and a summary of all assignments that could be obtained is given in Figure 4. A table of all chemical shifts recorded is available in the Supporting Information (Table S1).

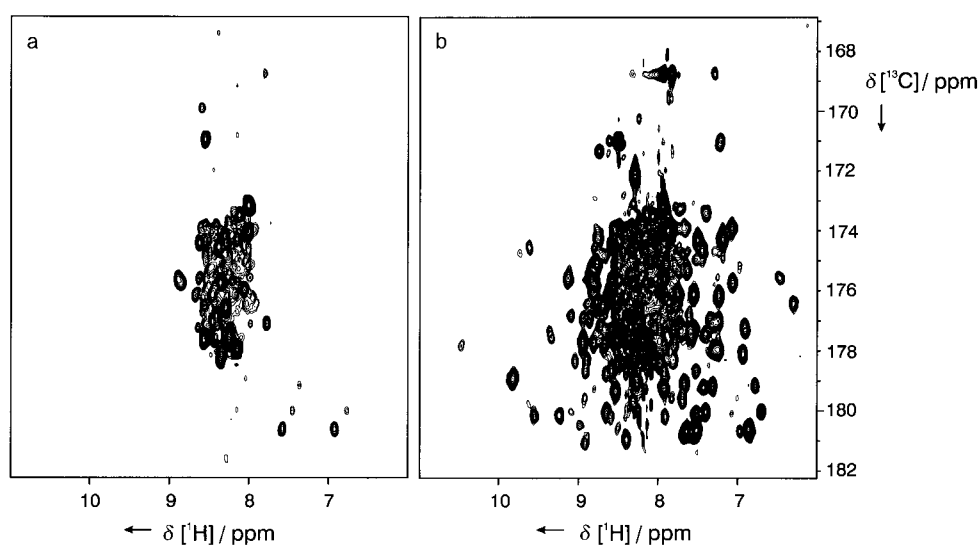


Figure 2. Comparison between the $^1\text{H},^{15}\text{N}$ projection of a conventional HNCO spectrum (a) and a TROSY HNCO spectrum (b) of $^2\text{H}/^{13}\text{C}/^{15}\text{N}$ -labeled BR. The advantage of the TROSY-based sequence is clearly visible. Many resonances of interest are not detected in the spectrum recorded with the conventional sequence.

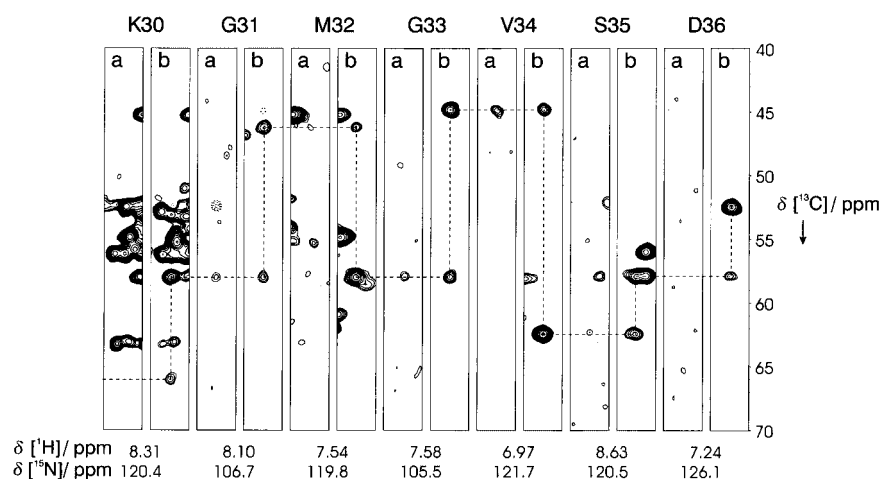


Figure 3. Strip plots of the HN(CO)CA (a) and HNCA (b) spectra of BR. The resonances of residues K30–D36 in the AB loop are shown. The signal-to-noise ratio for the peaks in the HN(CO)CA spectrum ranges from 5 to 10, and in the HNCA spectrum from 10 to 90. Sequential connectivities are indicated by dashed lines. Since HN(CO)CA is a less sensitive sequence than HNCA, the Ca correlations are sometimes not visible in the HN(CO)CA spectrum. In the HNCA spectrum, a distinction between inter- and intraresidue signals is often possible based on intensity.

Two sets of signals are present for residues 154–159 in the EF loop, which indicates an exchange process on a slow time scale. This result is particularly interesting since this region is not visible in the 1.55-Å X-ray structure and exhibits high B factors in other structures.^[11, 23]

The assignments were further used to obtain information on the dynamics of BR and to extract information on the secondary

structure. Qualitative information about the mobility of parts of the molecule was obtained from ^{15}N relaxation experiments, which were recorded at 600 MHz by using standard techniques.^[24] Information is available for a limited number of residues since relaxation times can only be retrieved for signals that do not overlap in an $^1\text{H}, ^{15}\text{N}$ correlation. A local correlation time can be estimated from the ratio of T_1 and T_2 relaxation rates^[25] (see Table S2 in the Supporting Information). The quality of the data, however, does not allow for a detailed quantitative analysis. Not unexpectedly, the C terminus shows the highest degree of mobility. This mobility corresponds to that of a small peptide, with an estimated correlation time of less than 3 ns. The highest T_1/T_2 ratios were measured for residues in the transmembrane helices. They result in an estimated correlation time of approximately 35 ns, which is in

excellent agreement with the data of Seigneuret et al.,^[13] who used viscosity measurements to obtain a correlation time of 33 ns for BR in DM micelles under comparable conditions. The mobility of the loop regions is in the range between that of the C terminus and that of the rigid parts of the molecule, with estimated correlation times between 10 and 30 ns. The EF loop shows the same mobility as the other loops, despite the fact that

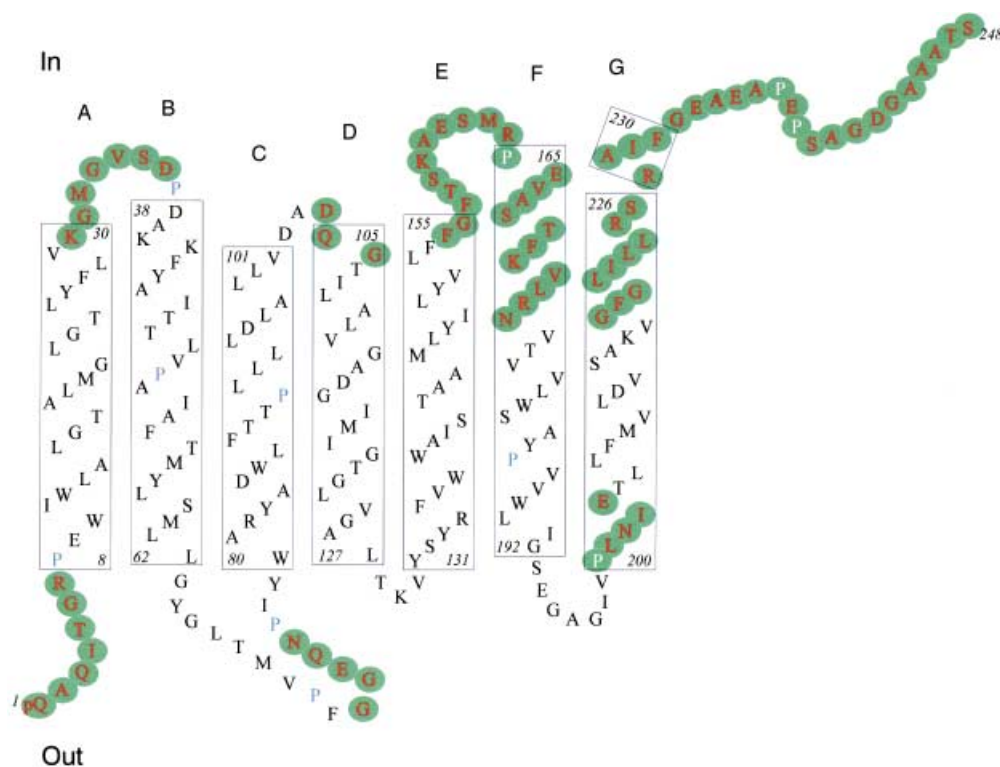


Figure 4. Schematic presentation of the unambiguously assigned residues. 33% of the residues (81 out of 248) could be assigned, mostly in loop regions. Two sets of signals are present for residues 154–159.

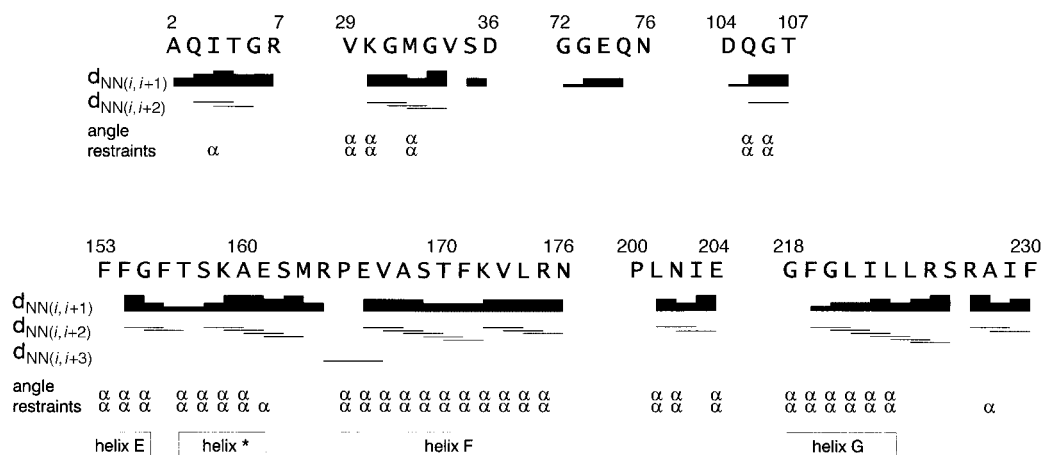


Figure 5. The secondary structure of BR obtained from secondary chemical shifts and NOEs. NOE signals are represented by lines whose thicknesses are related to the signal intensity. Deviation from *C α* random coil chemical shifts by more than 1.5 ppm and 2 ppm are indicated by α and $\alpha\alpha$, respectively. Positive deviations from *C α* random coil chemical shifts point to an α -helical structure. Residues 232–248 are not shown since no NOEs could be detected and only random coil carbon chemical shifts were observed. Regions of secondary structure that can be clearly identified are indicated at the bottom. The ends of helices E and G as well as the beginning of helix F can be reproduced. More importantly, a helical region (helix *) that is undefined in the high-resolution X-ray structure of BR is identified in the EF loop.

two sets of signals are observed. This is not surprising, however, since measurement of T_1 and T_2 relaxation times is not a suitable method to monitor slow exchange.

The secondary structure of a protein can be derived from carbon chemical shifts^[26] and from characteristic sequential NOEs.^[1] Information obtained for BR is depicted in Figure 5 for all residues that could be assigned. Since few $C\beta$ shifts were available, only the $C\alpha$ shifts were used to obtain structural information.^[27] The residues were classified according to their secondary chemical shifts as residues of stronger or weaker α -helical character and these results are given in Figure 5. In a highly deuterated protein, NOEs can only occur between amide protons. Nevertheless these NOEs can be indicative of secondary structure, in particular in helical regions of the molecule, as is also shown in Figure 5. The secondary structure prediction based on these data reproduces the helical parts of the transmembrane regions quite well. The data predict a helical region (residues 157–162) separated from the E and F helices by turns. This region corresponds to the EF loop not visible in the 1.55-Å X-ray structure.

In conclusion, we have shown that, given a suitably conditioned protein sample, high resolution NMR spectra can be obtained for loop regions of 7TM membrane proteins, which are of special importance for the understanding of membrane-protein–ligand interactions. Resonance assignment and subsequent extraction of structural and dynamic information is feasible. Quantification of the structural information extracted from the spectra of BR has been performed and structure calculations for the loops of BR based on those data are in progress.

Experimental Section

All NMR spectra were recorded at 323.5 K on Bruker spectrometers in standard configuration with an inverse triple resonance probe

equipped with three-axis self-shielded gradient coils. The relaxation experiments were recorded on a DRX600 spectrometer (600 MHz ^1H frequency) and all other experiments were recorded on a DMX750 spectrometer (750 MHz ^1H frequency). The following parameters were used for the individual experiments: 2D [^{15}N , ^1H] TROSY^[18] and 2D [^{15}N , ^1H] HSQC^[16]: 48 scans, data size $256(t_1) \times 1024(t_2)$ complex points, $t_{1\text{max}}$ (^{15}N) = 67.6 ms, $t_{2\text{max}}$ (^1H) = 82 ms; 3D [^{15}N , ^1H] TROSY-HNCA^[14]: 24 scans, data size $50(t_1) \times 62(t_2) \times 1024(t_3)$ complex points, $t_{1\text{max}}$ (^{13}C) = 8 ms, $t_{2\text{max}}$ (^{15}N) = 16.4 ms, $t_{3\text{max}}$ (^1H) = 82 ms; 3D [^{15}N , ^1H] TROSY-HN(CO)CA^[15]: 24 scans, data size $50(t_1) \times 62(t_2) \times 1024(t_3)$ complex points, $t_{1\text{max}}$ (^{13}C) = 8 ms, $t_{2\text{max}}$ (^{15}N) = 16.4 ms, $t_{3\text{max}}$ (^1H) = 82 ms; 3D [^{15}N , ^1H] TROSY-HNCO^[14]: 16 scans, data size $64(t_1) \times 64(t_2) \times 1024(t_3)$ complex points, $t_{1\text{max}}$ (^{13}C) = 21.2 ms, $t_{2\text{max}}$ (^{15}N) = 16.9 ms, $t_{3\text{max}}$ (^1H) = 82 ms; 3D [^{15}N , ^1H] TROSY-HN(CA)CO^[15]: 24 scans, data size $50(t_1) \times 60(t_2) \times 1024(t_3)$ complex points, $t_{1\text{max}}$ (^{13}C) = 16.6 ms, $t_{2\text{max}}$ (^{15}N) = 15.8 ms, $t_{3\text{max}}$ (^1H) = 82 ms; 3D [^{15}N , ^1H] TROSY-HNCACB^[15]: 24 scans, data size $50(t_1) \times 60(t_2) \times 1024(t_3)$ complex points, $t_{1\text{max}}$ (^{13}C) = 4 ms, $t_{2\text{max}}$ (^{15}N) = 15.8 ms, $t_{3\text{max}}$ (^1H) = 82 ms; 3D [^{15}N , ^1H] TROSY-HN(CO)CACB^[15]: 24 scans, data size $56(t_1) \times 62(t_2) \times 1024(t_3)$ complex points, $t_{1\text{max}}$ (^{13}C) = 4.5 ms, $t_{2\text{max}}$ (^{15}N) = 16.4 ms, $t_{3\text{max}}$ (^1H) = 82 ms; [^1H , ^1H]-NOESY–[^{15}N , ^1H]-TROSY^[28]: 8 scans, data size $128(t_1) \times 80(t_2) \times 1024(t_3)$ complex points, $t_{1\text{max}}$ (^1H) = 12.8 ms, $t_{2\text{max}}$ (^{15}N) = 21.1 ms, $t_{3\text{max}}$ (^1H) = 82 ms, NOESY mixing time 80 ms; [^1H , ^1H]-NOESY–[^{15}N , ^1H]-HSQC^[29]: 8 scans, data size $80(t_1) \times 128(t_2) \times 1024(t_3)$ complex points, $t_{1\text{max}}$ (^1H) = 8 ms, $t_{2\text{max}}$ (^{15}N) = 33.8 ms, $t_{3\text{max}}$ (^1H) = 82 ms, NOESY mixing time 80 ms; [^{15}N , ^1H]-HMQC-NOESY–[^{15}N , ^1H]-HSQC^[30]: 24 scans, data size $64(t_1) \times 64(t_2) \times 1024(t_3)$ complex points, $t_{1\text{max}}$ (^{15}N) = 16.9 ms, $t_{2\text{max}}$ (^{15}N) = 16.9 ms, $t_{3\text{max}}$ (^1H) = 82 ms, NOESY mixing time 50 ms. Recycle delays of 2 s were used. Prior to Fourier transformation, a Gaussian window was applied in the acquisition dimension and a 90° -shifted squared sine bell window in the indirect dimensions.

Parameters used in the T_1 and T_2 relaxation experiments^[24] were: data size $128(t_1) \times 1024(t_2)$ complex points, $t_{1\text{max}}$ (^{15}N) = 21.2 ms, $t_{2\text{max}}$ (^1H) = 51.2 ms. The number of scans was 16 for the T_1 and 24 for the T_2 measurements. 11 time points were acquired for each T_1 decay: 5, 25, 50, 75, 100, 150, 200, 300, 400, 1000, 2500 ms. Likewise, 11 time points were acquired for each T_2 decay: 5, 10, 20, 30, 40, 50, 100, 150, 200, 250, 300 ms.

Support from the Forschungsinstitut für Molekulare Pharmakologie is gratefully acknowledged. M.S. was supported by the DFG Graduiertenkolleg GRK 80 "Modellstudien". The authors thank Wolfgang Bernel for helpful discussions regarding the setup of the TROSY experiments, Hartmut Oschkinat for his continuous encouragement, and Karen Zierler for carefully reading the manuscript.

- [1] K. Wüthrich, *NMR of Proteins and Nucleic Acids*, Wiley, New York, 1986.
- [2] a) G. T. Montelione, G. Wagner, *J. Magn. Reson.* 1990, 87, 183–188; b) L. E. Kay, M. Ikura, R. Tschudin, A. Bax, *J. Magn. Reson.* 1990, 89, 496–514; c) G. M. Clore, A. M. Gronenborn, *Prog. Nucl. Magn. Reson. Spectrosc.* 1991, 23, 43–92; d) M. Sattler, J. Schleucher, C. Griesinger, *Prog. Nucl. Magn. Reson. Spectrosc.* 1999, 34, 93–158.
- [3] L. P. McIntosh, F. W. Dahlquist, *Q. Rev. Biophys.* 1990, 23, 1–38.
- [4] a) K. H. Gardner, L. E. Kay, *Biol. Magn. Reson.* 1999, 16, 27–74; b) B. T. Farmer II, R. A. Venters, *Biol. Magn. Reson.* 1999, 16, 75–120.
- [5] a) K. Pervushin, R. Riek, G. Wider, K. Wüthrich, *Proc. Natl. Acad. Sci. USA* 1997, 94, 12366–12371; b) K. Pervushin, *Q. Rev. Biophys.* 2000, 33, 161–197.
- [6] A. Arora, L. K. Tamm, *Curr. Opin. Struct. Biol.* 2001, 11, 540–547.
- [7] a) A. Arora, F. Abildgaard, J. H. Bushweller, L. K. Tamm, *Nat. Struct. Biol.* 2001, 8, 334–338; b) C. Fernandez, K. Adeishvili, K. Wüthrich, *Proc. Natl. Acad. Sci. USA* 2001, 98, 2358–2363; c) C. Fernandez, C. Hilty, S. Bonjour, K. Adeishvili, K. Pervushin, K. Wüthrich, *FEBS Lett.* 2001, 504, 173–178.
- [8] a) J. K. Lanyi, *Biochim. Biophys. Acta.* 2000, 1460, 1–3 and references cited therein; b) U. Haupts, J. Tittor, D. Oesterhelt, *Annu. Rev. Biophys. Biomol. Struct.* 1999, 28, 367–99; c) D. Oesterhelt, *Curr. Opin. Struct. Biol.* 1998, 8, 489–500; d) D. Oesterhelt, W. Stoeckenius, *Nature (London), New Biol.* 1971, 233, 149–152.
- [9] a) J. Wess, *FASEB J.* 1997, 11, 346–354; b) H. G. Dohlman, J. Thorner, M. G. Caron, R. J. Lefkowitz, *Annu. Rev. Biochem.* 1991, 60, 653–688.
- [10] K. Palczewski, T. Kumasaka, T. Hori, C. A. Behnke, H. Motoshima, B. A. Fox, I. Le Trong, D. C. Teller, T. Okada, R. E. Stenkamp, M. Yamamoto, M. Miyano, *Science* 2000, 289, 739–745.
- [11] H. Luecke, B. Schobert, H.-T. Richter, J.-P. Cartailler, J. K. Lanyi, *J. Mol. Biol.* 1999, 291, 899–911.
- [12] a) H. Patzelt, A. S. Ulrich, H. Egbringhoff, P. Dux, J. Ashurst, B. Simon, H. Oschkinat, D. Oesterhelt, *J. Biomol. NMR* 1997, 10, 95–106; b) M. Kolbe, PhD thesis, Ludwig-Maximilians-University Munich, 2001.
- [13] M. Seigneuret, J. M. Neumann, J. L. Rigaud, *J. Biol. Chem.* 1991, 266, 10066–10069.
- [14] M. Salzmann, K. Pervushin, G. Wider, H. Senn, K. Wüthrich, *Proc. Natl. Acad. Sci. USA* 1998, 95, 13585–13590.
- [15] M. Salzmann, G. Wider, K. Pervushin, H. Senn, K. Wüthrich, *J. Am. Chem. Soc.* 1999, 121, 844–848.
- [16] V. Sklenar, M. Piotto, R. Leppik, V. Saudek, *J. Magn. Reson. Ser. A* 1993, 102, 241–245.
- [17] a) A. G. Palmer, J. Cavanagh, P. E. Wright, M. Rance, *J. Magn. Reson.* 1991, 93, 151–170; b) L. E. Kay, P. Keifer, T. Saarinen, *J. Am. Chem. Soc.* 1992, 114, 10663–10665.
- [18] K. V. Pervushin, G. Wider, K. Wüthrich, *J. Biomol. NMR* 1998, 12, 345–348.
- [19] M. J. Pettei, A. P. Yudd, K. Nakanishi, R. Henselman, W. Stoeckenius, *Biochemistry* 1977, 16, 1955–1959; b) G. S. Harbison, S. O. Smith, J. A. Pardo, C. Winkel, J. Lugtenburg, J. Herzfeld, R. Mathies, R. G. Griffin, *Proc. Natl. Acad. Sci. USA* 1984, 81, 1706–1709; c) S. O. Smith, A. B. Myers, J. A. Pardo, C. Winkel, P. P. J. Mulder, J. Lugtenburg, R. Mathies, *Proc. Natl. Acad. Sci. USA* 1984, 81, 2055–2059; d) P. Scherrer, M. K. Mathew, W. Sperling, W. Stoeckenius, *Biochemistry* 1989, 28, 829–834.
- [20] a) J. P. Loria, M. Rance, A. G. Palmer III, *J. Magn. Reson.* 1999, 141, 180–184; b) P. Permi, A. Annala, *J. Biomol. NMR* 2001, 20, 127–133.
- [21] S. Grzesiek, A. Bax, *J. Biomol. NMR* 1993, 3, 185–204.
- [22] J. Cavanagh, W. J. Fairbrother, A. G. Palmer III, N. J. Skelton, *Protein NMR Spectroscopy*, Academic Press, San Diego 1996.
- [23] a) H. Belrhali, P. Nollert, A. Royant, C. Menzel, J. P. Rosenbusch, E. M. Landau, E. Pebay-Peyroula, *Structure Fold. Des.* 1999, 7, 909–917; b) L. O. Essen, R. Siegert, W. D. Lehmann, D. Oesterhelt, *Proc. Natl. Acad. Sci. USA* 1998, 95, 11673–11678.
- [24] N. A. Farrow, R. Muhandiram, A. U. Singer, S. M. Pascal, C. M. Kay, G. Gish, S. E. Shoelson, T. Pawson, J. D. Forman-Kay, L. E. Kay, *Biochemistry* 1994, 33, 5984–6003.
- [25] a) D. Fushman, R. Weisemann, H. Thüring, H. Rüterjans, *J. Biomol. NMR* 1994, 4, 61–78; b) M. R. Gryk, R. Abseher, B. Simon, M. Nilges, H. Oschkinat, *J. Mol. Biol.* 1998, 280, 879–896.
- [26] S. Spera, A. Bax, *J. Am. Chem. Soc.* 1991, 113, 5490–5492.
- [27] P. Luginbühl, T. Szyperski, K. Wüthrich, *J. Magn. Reson. Ser. B* 1995, 109, 229–233.
- [28] G. Zhu, Y. Xia, K. H. Sze, X. Yan, *J. Biomol. NMR* 1999, 14, 377–381.
- [29] A. Bax, S. Grzesiek in *NMR of Proteins* (Eds.: G. M. Clore, A. M. Gronenborn), CRC Press, Boca Raton, FL, 1993, pp. 36.
- [30] a) M. Ikura, A. Bax, G. M. Clore, A. M. Gronenborn, *J. Am. Chem. Soc.* 1990, 112, 9020–9022; b) T. Frankiel, C. Bauer, M. D. Carr, B. Birdsall, J. Feeney, *J. Magn. Reson.* 1990, 90, 229.

Received: March 15, 2002 [Z 380]

The First Orally Active Low Molecular Weight Agonists for the LH Receptor: Thienopyr(im)idines with Therapeutic Potential for Ovulation Induction

N. C. R. van Straten,^{*,[a]} G. G. Schoonus-Gerritsma,^[a] R. G. van Someren,^[a] J. Draaijer,^[a] A. E. P. Adang,^[a] C. M. Timmers,^[b] R. G. J. M. Hanssen,^[c] and C. A. A. van Boeckel^[a]

KEYWORDS:

G-protein-coupled receptors · medicinal chemistry · nitrogen heterocycles · receptors · structure–activity relationships

The gonadotropins, a class of glycoproteins with an average molecular weight of 30 kD, play a pivotal role in human reproduction. Follicle stimulating hormone (FSH), for example, causes ovarian follicle maturation in women and is involved in spermatogenesis in men. Luteinizing hormone (LH) is responsible for ovulation induction in women and controls testosterone production in men. Finally, human choriogonadotropin (hCG) maintains the early stages of a pregnancy.^[1] All gonadotropins consist of a common α subunit and a hormone-specific

[a] Dr. N. C. R. van Straten, G. G. Schoonus-Gerritsma, R. G. van Someren, J. Draaijer, Dr. A. E. P. Adang, Prof. Dr. C. A. A. van Boeckel
Lead Discovery Unit
N.V. Organon
PO Box 20
5340 BH Oss (The Netherlands)
Fax: (+31)4126-63508
E-mail: nicole.vanstraten@organon.com

[b] Dr. C. M. Timmers
Dept. of Medicinal Chemistry
N.V. Organon (The Netherlands)

[c] Dr. R. G. J. M. Hanssen
Dept. of Pharmacology
Research and Development
N.V. Organon (The Netherlands)